Long Waves in Parallel Flow in Hele-Shaw Cells

M. Zeybek and Y. C. Yortsos
Department of Chemical Engineering, University of Southern California, Los Angeles, California 90089-1211
(Received 11 January 1991)

The evolution of fluid interfaces in parallel flow in Hele-Shaw cells is studied theoretically and experimentally in the limit of large capillary number. It is shown that such interfaces support wave motion, the amplitude of which for long waves is governed by a set of Korteweg–de Vries and Airy equations. Experiments conducted in a long Hele-Shaw cell validate the theory in the symmetric case.

PACS numbers: 47.15.Hg, 47.55.Mh

The flow of two immiscible fluids in a Hele-Shaw cell has been a subject of great interest. The majority of studies have focused on frontal displacement, particularly on viscous fingering [1–3] (VF). This is readily understood in view of the interesting problems in the high-N_{ca} limit [4], the relation of VF to Laplacian growth [5], and the implications to oil recovery [6]. In contrast, little attention has been paid to the dynamics of interfaces parallel to the main flow direction. Although lacking the richness of frontal motion, parallel flow is nonetheless interesting. Parallel flow is the theoretical limit of fully developed fingers (e.g., the Saffman-Taylor finger). Even in the absence of capillarity, this regime is of great interest, especially for finite viscosity ratio [7]. In porous media, parallel flow develops in thin reservoirs, under the conditions of vertical flow equilibrium [8]. Finally, interfaces parallel to the main flow may support motion similar to shallow water waves, the Laplace equation being the field equation in both cases. The latter possibility has obvious interests of its own and forms the subject of this paper.

We study the interfaces between two immiscible and incompressible fluids of different viscosities in the parallel flow schematic of Fig. 1. The Hele-Shaw cell is horizontal and has half width W. For the fluids to flow in parallel requires flat interfaces; thus the absence of transverse pressure gradients. This further necessitates that the two velocities are related, $\mu_b q_b = \mu_a q_a \equiv Q$, where subscript a denotes the "inner" fluid. Under this condition, steady-state interfaces are flat. We denote their normalized positions by λ_1 and λ_2 ($-1 \le \lambda_2 \le \lambda_1 \le 1$), where transverse lengths are scaled with the half width W, and define the viscosity ratio in the usual manner, $M \equiv \mu_b/\mu_a$. Of significant interest below is the symmetric case ($\lambda_1 = -\lambda_2$). We may note that the Saffman-Taylor finger corresponds to $\lambda_1 = -\lambda_2 = \frac{1}{2}$, $M = \infty$.

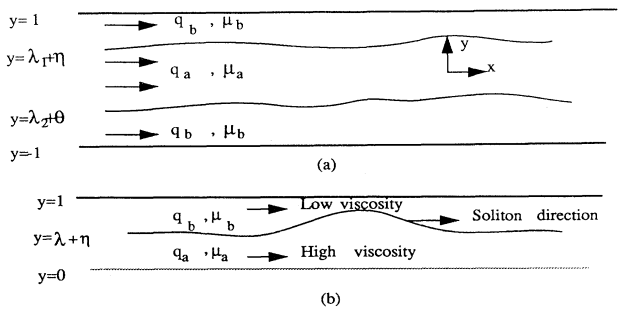

FIG. 1. Flow geometry for (a) nonsymmetric and (b) symmetric cases.

To study interface dynamics, we first derive the linear dispersion relation using normal modes ($e^{i(\omega t - kx)}$), where we scale time by L/q_a and streamwise lengths by L. A compact result is obtained in the symmetric case ($\lambda_1 = -\lambda_2$ and $\eta = -\theta$, where η and θ are scaled amplitudes),

$$\omega = 2\frac{k\sinh k}{(1+M)\sinh k + (1-M)\sinh k(1-2\lambda_1)} + \frac{i}{6N'_{ca}}\frac{k^3\sinh(k\lambda_1)\sinh k(1-\lambda_1)}{(1+M)\sinh k + (1-M)\sinh k(1-2\lambda_1)}. \quad (1)$$

It is noted that in the above, capillarity first enters at $O(k^4)$. For long waves (small k) and for a sufficiently large value of the modified [2] capillary number, $N'_{ca} = q_a\mu_a L^2/\gamma b^2$, capillarity can be neglected (but see also Ref. [9]). Here, b denotes the cell spacing. Then, the rate of growth is strictly real and the wave speed $c \equiv \omega/k$ is

$$c = c_0\left[1 - \frac{k^2}{3}\frac{(M-1)\lambda_1(1-2\lambda_1)(1-\lambda_1)}{1-\lambda_1+\lambda_1 M} + \cdots\right], \quad (2)$$

where $c_0 = 1/(1-\lambda_1+\lambda_1 M)$. For $M \neq 1$, the above predicts dispersive waves [10], i.e., waves with different wavelength have different speed. Nondispersive waves are predicted for $M = 1$ (any λ_1) and for $\lambda_1 = \frac{1}{2}$ (any M). For the specific Saffman-Taylor finger, however, they have an infinitesimal velocity ($M \gg 1$).

A similar analysis for the nonsymmetric case ($\lambda_1 \neq -\lambda_2$) leads to a complicated expression, which has the following simple asymptotic behavior. Two solutions (corresponding to two interface modes) exist,

$$\omega_m = k(x_{0,m} + x_{2,m}k^2 + \cdots), \quad m = 1,2, \quad (3)$$

where $x_{0,1}=+1/M$, $x_{0,2}=+2/\Delta$,

$$x_{2,1}=(M-1)(\lambda_1-1)(\lambda_2+1)(\lambda_1-\lambda_2)/M^2(2+\lambda_2-\lambda_1),$$

$$x_{2,2}=4(M-1)(\lambda_1-\lambda_2)(1+\lambda_2-\lambda_1)[(\lambda_2+1)^2+(\lambda_1-1)^2+(\lambda_2+1)(\lambda_1-1)]/3\Delta^2(2+\lambda_2-\lambda_1),$$

and where $\Delta\equiv 2+(M-1)(\lambda_1-\lambda_2)$. As in (2), dispersive waves are predicted for $M\neq 1$.

Subsequently, we consider the nonlinear evolution of small-amplitude (ϵ), long-wave (δ) disturbances. We take $\epsilon=O(\delta^2)$, $\delta=W/L$, and ϵ and $\delta\ll 1$. We outline the key steps of the approach that closely follows Ref. [11]. In each region, the Laplace equation is satisfied [2]

$$\delta^2\phi_{ixx}+\phi_{iyy}=0,\quad i=a,1,2, \tag{4}$$

where subscripts 1 and 2 denote the "upper" and "lower" regions of fluid b, respectively [Fig. 1(a)]. Across each interface, pressure and normal fluxes are continuous. For the upper interface, we obtain $\phi_1=\phi_a$ and

$$\delta^2(\phi_{ix}-1)\eta_x-\phi_{iy}=\delta^2M(\phi_{ax}-1)\eta_x-M\phi_{ay},\quad i=1, \tag{5}$$

$$\delta^2[\eta_t-\eta_x(\phi_{ax}-1)]=-\phi_{ay}. \tag{6}$$

Similar equations with η replaced by θ hold for the lower interface. Then the following asymptotic expansions are taken, $\phi_i=\epsilon\phi_{i,0}+\epsilon\delta^2\phi_{i,1}+\epsilon\delta^4\phi_{i,2}+\cdots$, for $i=a,1,2$, $\eta=\epsilon\eta_0+\epsilon^2\eta_1+\cdots$, and $\theta=\epsilon\theta_0+\epsilon^2\theta_1+\cdots$, and two-timing ($t$, $\tilde{t}=\epsilon t$) is introduced. By eliminating secular terms at first order and after lengthy calculations, the following set of Korteweg-de Vries and Airy equations is obtained:

$$V_{\tilde{t}}-\frac{(M-1)}{M\Delta}a_1V_{\xi\xi\xi}=0, \tag{7}$$

$$U_{\tilde{t}}-\frac{4(M-1)}{\Delta^2}(2+\lambda_2-\lambda_1)UU_\sigma-\frac{(M-1)\kappa^2}{M\Delta}a_2U_{\sigma\sigma\sigma}=0. \tag{8}$$

Here, V and U are linearly related to the leading terms of the interface amplitude η_0 and θ_0 [Fig. 1(a)]:

$$V\equiv-[(1+\lambda_2)\eta_0+(1-\lambda_1)\theta_0]/(2-\lambda_1+\lambda_2),$$

$$U\equiv(\eta_0-\theta_0)/(2-\lambda_1+\lambda_2).$$

Variable U denotes the net transverse displacement of fluid a. The parameters in (7) and (8) are consistent with (3) since $a_m=M\Delta x_{2,m}/(M-1)$, $m=1,2$, and $\delta=\kappa\sqrt{\epsilon}$. The two equations have been decoupled using two different moving coordinates, $\xi\equiv x-t/M$ and $\sigma\equiv x-2t/\Delta$.

From (7) and (8) we note the following: (i) Translational motion occurs for $M=1$; (ii) there are two long-wave speeds, $1/M$ and $2/\Delta$, both decreasing to zero at large M; (iii) the dispersive term in the KdV equation vanishes for $1+\lambda_2-\lambda_1=0$ (which, in the symmetric case, coincides with the Saffman-Taylor condition, $\lambda_1=\frac{1}{2}$); (iv) antisymmetric disturbances ($\eta=\theta$) are governed by the linear Airy equation alone; (v) the symmetric problem ($\lambda_1=-\lambda_2$ and $\eta=-\theta$) is governed by the KdV equation alone. The latter also pertains to the experiments below [Fig. 1(b)]. In that case, we recast for simplicity (8) in terms of the original variables η, x, t, and c_0,

$$\eta_t+c_0\eta_x-2(M-1)c_0^2\eta\eta_x+\epsilon(c_0^2/3)\kappa^2(M-1)\lambda(1-2\lambda)(1-\lambda)\eta_{xxx}=0. \tag{9}$$

Equation (9) can be interpreted as follows: Because of parallel flow, an initial disturbance travels with a long-wave speed c_0. The latter always lies between the velocities of the two fluids (e.g., $1<c_0<1/M$ for $M<1$). For an observer traveling with speed c_0 the fluid flow is countercurrent, the lower-viscosity fluid flowing towards the right and the higher-viscosity one towards the left in the schematic of Fig. 1(b). It must be recalled that in the Hele-Shaw context, viscous shear is not relevant to long waves. Because of unequal viscosities, the long-wave disturbances also disperse, to the left if $(M-1)(1-2\lambda)>0$, and to the right, otherwise. We note that shorter-wavelength dispersion, although possible, is likely to be damped by capillarity and wettability effects. Sustained wave propagation is possible if amplitudes are small and the nonlinearity is weak. Strong nonlinear effects must be excluded. They violate parallel-flow conditions and are likely to lead to frontal motion and viscous fingering. Nonetheless, weakly nonlinear waves also tend to break, to the left if $(M-1)\eta>0$, and to the right, otherwise. For the positive disturbance of Fig. 1(b), dispersion will oppose breaking if $1-2\lambda<0$. Under this condition, a permanent form wave would develop that propagates to the left or to the right, depending on whether $M>1$ or $M<1$, respectively. Analogous conclusions can be drawn for all other possibilities.

To test the theory, a long and narrow Hele-Shaw cell was constructed consisting of two Plexiglass plates 0.5 in. thick, of dimensions 220 cm×27 cm, separated by a rubber spacer 0.08 cm thick and 10 cm wide. The setup consists of the cell, two peristaltic pumps, and video equipment. Although other fluid pairs were also used, the experiments reported here were conducted with mineral oil and glycerol-water solution, with viscosities 170 and 860 cP, respectively, and with values of the modified capillary number of order 10^2. For substantially lower values of N'_{ca}, sustained propagation was not observed, thus confirming the importance of capillarity at low N'_{ca}. The experiments involved only one interface [Fig. 1(b)], pertaining to the symmetric case. Because (7) and (8)

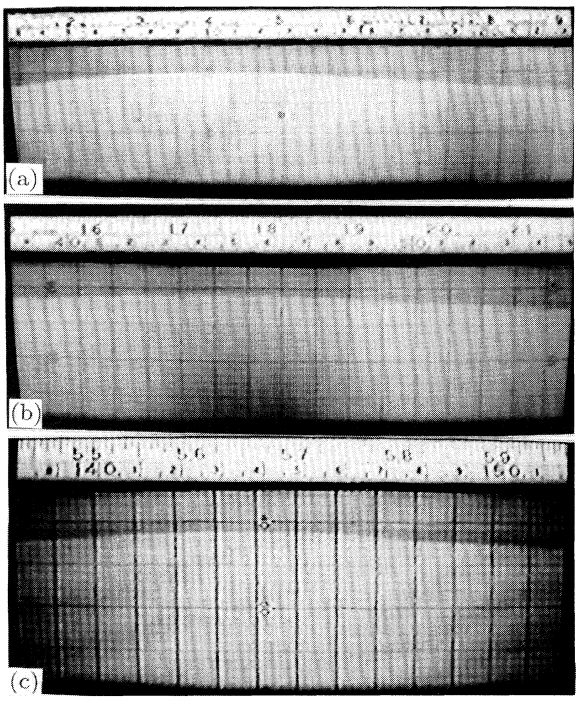

FIG. 2. Single solitary wave. (a) Initial condition; (b),(c) subsequent stages.

are invariant to the change $\lambda_1 \rightarrow 1+\lambda_2$, $\eta \rightarrow \theta$, $M \rightarrow 1/M$ (note also the rescaling of time), we may view the flow as the top half of a symmetric problem, the lower fluid being fluid a. In our experiments, this was the more viscous fluid ($M=0.2$).

Conducting the flow experiments consists of (i) establishing a flat interface and parallel flow conditions ($\mu_b q_b = \mu_a q_a$) and (ii) monitoring the motion of disturbances initiated by interrupting momentarily the flow of one fluid. Existence of solitons can be tested by comparison with simulation, but more conveniently by looking for key properties [10]: (i) Arbitrary disturbances evolve into one or more solitons and dispersive waves; (ii) the speed of a soliton increases with an increase in amplitude; and (iii) solitons regain their identity after interaction. Typical results from still pictures taken from a videotape are shown below. It must be pointed out that once the disturbance exits the cell, the original interface is recovered; thus the experiments can be easily reproduced.

Figure 2(a) shows a typical initial disturbance imposed on the parallel interface. Upon restoration of the flow, the disturbance moves forward, while also starting to develop into a wave of constant shape. This is followed by a wiggly interface of small amplitude and short wavelength. Typically, this wave takes a permanent form after traveling about 45 cm [Fig. 2(b)], and appears to possess all the characteristics of a soliton. Its amplitude is different from the initial one and remains constant for a substantial distance traveled [Fig. 2(c)] (as long as 150 cm, beyond which end effects become appreciable). A simulation of this run based on the technique of Ref. [12] is shown in Fig. 3. Good agreement between theory and experiment is obtained, despite the ambiguity on the suitability of the initial condition in the simulation (due to the flow interruption). We note that features typically associated with soliton and dispersive waves are suppressed in the scales of Fig. 3, that match the experiment. We illustrate this point by replotting the profile in the inset with different scales. We must add that dispersive waves were not obtained to our satisfaction. A noisy interface of small wavelength and amplitude did form soon after the main wave evolved. However, we suspect that wettability and surface tension become predominant in its subsequent development.

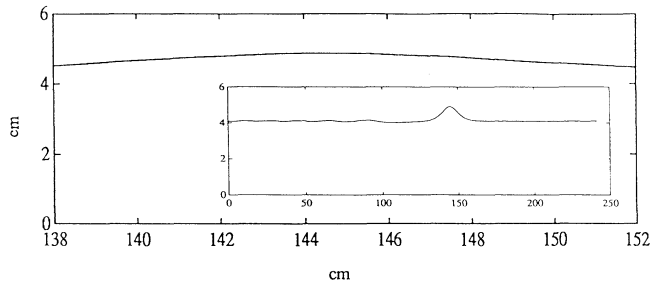

FIG. 3. Numerical simulation of Fig. 2(c). Inset: Profile in different scales.

Wave interaction is shown in Fig. 4. The two waves were created by sequentially introducing two disturbances of different amplitude. The second is of higher amplitude and evolves into a faster soliton that eventually overtakes the preceding one. After interaction, tall and short soli-

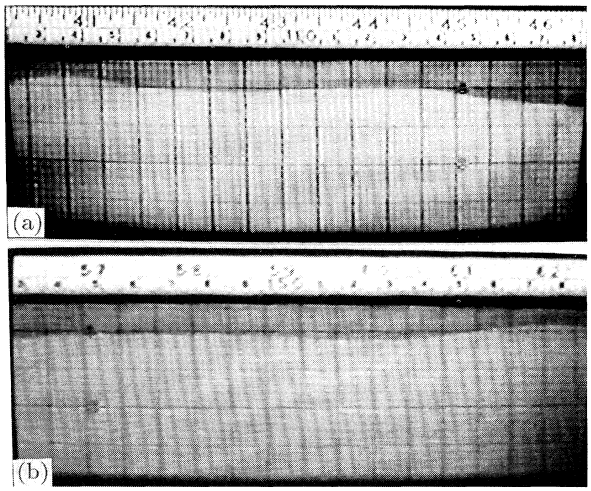

FIG. 4. Two solitary waves (a) before and (b) after interaction.

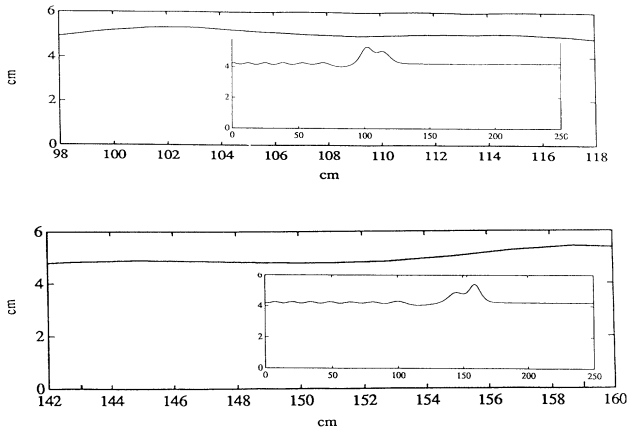

FIG. 5. Numerical simulation of Fig. 4. Inset: Profile in different scales.

tons reappear, but in reverse order, and they propagate with their original speed [Fig. 4(b)]. The corresponding numerical simulations are shown in Fig. 5.

A variety of other conditions (not shown because of space limitation) were also investigated and found consistent with the theory. Two solitary waves of different amplitudes resulted from a longer-wavelength initial disturbance, as expected. Comparison with the numerical simulations was also satisfactory in this case. Short-wave disturbances dissipated shortly after their onset, as also predicted. For solitons that propagate in the negative σ direction ($\lambda < \frac{1}{2}$), dispersive waves should proceed them in a fixed frame of reference. Such were noticed, although the above remarks on wettability effects apply here as well. We must point out that because of wettability effects, all our experiments were limited to disturbances in the direction of drainage (nonwetting displacing wetting). For $M = 1$, constant wave speed and motion independent of the amplitude are expected. These features were indeed observed for nearly equal-viscosity fluids. Furthermore, for $M \sim 1$, large-amplitude waves did not break, in contrast to every other case studied.

In summary, in this paper we presented an analysis of the wave motion of the interface of immiscible fluids in viscous-dominated parallel flow in a long Hele-Shaw cell. Small-amplitude, long-wavelength disturbances were shown to be governed by KdV and Airy equations. For the symmetric problem, experimental evidence was supportive of the theory, including the propagation of solitary waves.

This work was partly supported by DOE Contract No. DE-FG19-87BC14126, the contribution of which is gratefully acknowledged.

[1] P. G. Saffman and G. I. Taylor, Proc. Roy, Soc. London A **245**, 312–329 (1958).

[2] D. Bensimon, L. P. Kadanoff, S. Liang, B. I. Shraiman, and C. Tang, Rev. Mod. Phys. **58**, 977 (1986); G. M. Homsy, Annu. Rev. Fluid Mech. **19**, 271–311 (1987).

[3] L. Paterson, J. Fluid Mech. **113**, 513 (1981); G. Tryggvason and H. Aref, J. Fluid Mech. **136**, 1 (1983).

[4] R. Combescot, T. Dombre, V. Hakim, Y. Pomeau, and A. Pumir, Phys. Rev. Lett. **56**, 2036 (1986); B. Shraiman, Phys. Rev. Lett. **56**, 2028 (1986).

[5] P. Pelcé, *Dynamics of Curved Fronts* (Academic, New York, 1988).

[6] J. Feder, *Fractals* (Plenum, New York, 1988); R. Lenormand, Proc. Roy. Soc. London A **23**, 159 (1989).

[7] M. J. King and H. Sher, Phys. Rev. A **41**, 874 (1990); J. Lee, A. Coniglio, and H. E. Stanley, Phys. Rev. A **41**, 4589 (1990).

[8] K. H. Coats, J. R. Dempsey, and J. H. Henderson, Soc. Pet. Eng. J. **1971**, 63; F. J. Fayers and T. M. J. Newley, Soc. Pet. Eng. Reservoir Eng. **1988**, 542.

[9] T. Maxworthy, Phys. Rev. A **39**, 5863 (1989).

[10] M. J. Ablowitz and H. Segur, *Solitons and Inverse Scattering Transform* (Society for Industrial and Applied Mathematics, Philadelphia, 1981); P. G. Drazin and R. J. Johnson, *Solitons: An Introduction* (Cambridge Univ. Press, Cambridge, 1989).

[11] J. Kevorkian and J. D. Cole, *Perturbation Methods in Applied Mathematics* (Springer-Verlag, Berlin, 1981), Vol. 34.

[12] R. B. Fornberg and G. B. Whitham, Philos. Trans. Roy. Soc. London A **289**, 373–404 (1978).

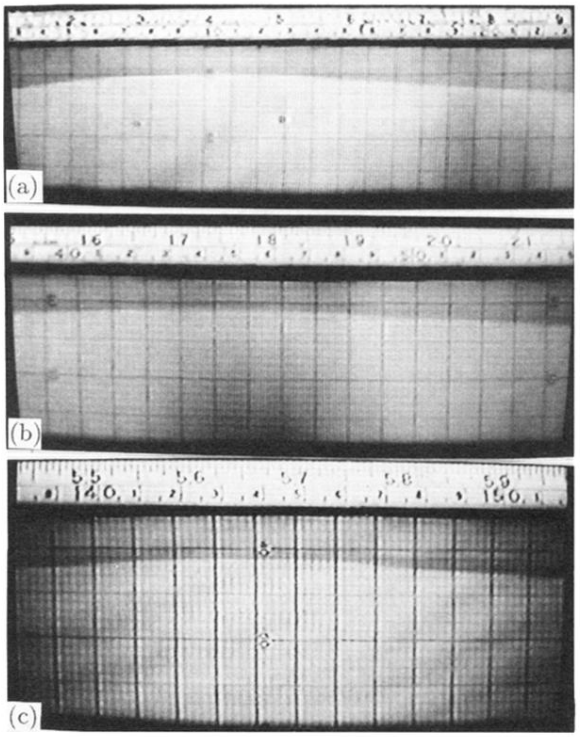

FIG. 2. Single solitary wave. (a) Initial condition; (b),(c) subsequent stages.

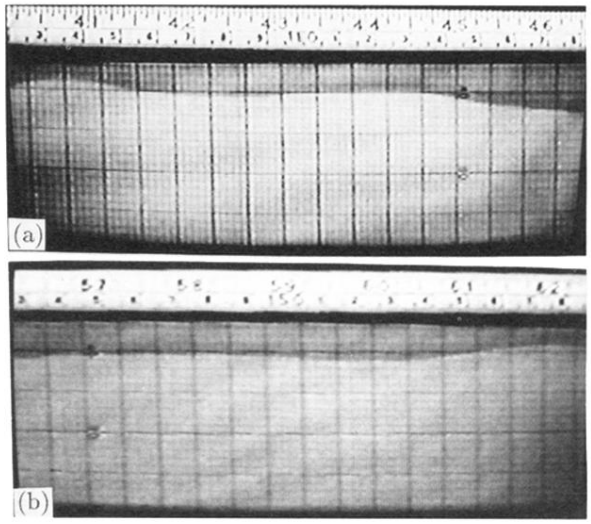

FIG. 4. Two solitary waves (a) before and (b) after interaction.